Belousov-Zhabotinskii Reaction

Zachariah Sachs (with Jeff Montgomery)

June 4, 2013

1 Purpose

In this laboratory exercise, we explore the oscillatory kinetics manifest in temporal and spatial complexity of the Belousov-Zhabotinskii reaction through analysis of spectral data over time for the seemingly homogeneous three-dimensional process and of wave propagation in the inhomogeneous thin-layer two-dimensional case.

2 Theory and Methods

2.1 Complexity, Oscillations, and the Lotka Mechanism

Many important processes in biology and elsewhere depend on dynamic behavior which does not proceed monotonically toward equilibrium and which is sensitive to spatial inhomogeneities and concentration gradients. Really, any cyclic biochemical process, such as glycolysis in yeast, must respond to the chemical environment to fulfill the needs of a living organism. These reactions must not overconsume resources or overproduce products, yet a nonzero chemical potential is necessary to do work. Complexities may be localized to a single cell, as in the self-replication of RNA, or coordinated through a much larger organism, as needed to maintain the regular beating of a heart. Obviously, these chemical processes must provide amplification and feedback in the right location and on an appropriate timescale to function properly.

Alfred Lotka hypothesized the following set of reactions which would show temporal oscillations of intermediates X and Y in the overall reaction $A \longrightarrow P$:

$$A + X \xrightarrow{k_1} 2X \tag{1}$$

$$X + Y \xrightarrow{k_2} 2Y \tag{2}$$

$$Y \xrightarrow{k_3} P. \tag{3}$$

Reactions (1) and (2) are autocatalytic, and reactions (2) and (3) use reactants from (1) and (2) to provide negative feedback. The rate equations for this

system are then

$$\frac{d[A]}{dt} = -k_1[A][X] \tag{4}$$

$$\frac{d[X]}{dt} = k_1[A] - k_2[X][Y] \tag{5}$$

$$\frac{d[Y]}{dt} = k_2[X][Y] - k_3[Y] \tag{6}$$

$$\frac{d[P]}{dt} = k_3[Y]. \tag{7}$$

These differential equations are nonlinear as a result of the feedback in the system, and complexity in the form of oscillations will likely result.

2.2 The Field-Körös-Noyes Mechanism for the Belousov-Zhabotinskii Reaction

The Belousov-Zhabotinskii (BZ) reaction was discovered by Belousov, reproduced by Zhabotinskii, and a model for its mechanism was proposed by Field, Körös, and Noyes. In a well-stirred solution, the three-dimensional case, the electrochemical potential oscillates displaying homogeneous color changes as the reaction cycles. In unstirred solution, the two-dimensional case, diffusion of reaction intermediates produces spatial concentration gradients which propogate and are visible as a color wave.

Like the Lotka Mechanism, concentrations of the intermediates in the BZ reaction oscillate as the concentration of the products proceeds to equilibrium. Bromine-containing intermediates and cerium(III/IV) catalysts aid in the overall oxidation by bromate, BrO_3^-, of malonic acid, $CH_2(COOH)_2$, to carbon dioxide, water, and bromide. The Field-Körös-Noyes (FKN) mechanism for the BZ reaction involves nine key steps and includes feedback and autocatalysis[1]. The FKN mechanism is simplified in the "Oregonator" scheme,

$$A + Y \xrightarrow{k_1} X \tag{8}$$

$$X + Y \xrightarrow{k_2} P \tag{9}$$

$$B + X \xrightarrow{k_3} 2X + Z \tag{10}$$

$$2X \xrightarrow{k_4} Q \tag{11}$$

$$Z \xrightarrow{k_5} Y, \tag{12}$$

where $A = B$=BrO_3^- is substrate, X=$HBrO_2$, Y=Br^-, and Z=Ce^{4+} are intermidiates, and P and Q are products. Note equation (10) is coupled to the other four equations; it appears to be the crux of feedback in this system, and is also the only autocatalytic step. This mechanism is clearly more complex than the Lotka mechanism, and therefore could either have more controlled or more

[1]The key reactions of the FKN mechanism, included in the procedure, are suppressed here.

chaotic behavior. The kinetics for this system are then given by the differential equations

$$\frac{d[X]}{dt} = k_1[A][Y] - k_2[X][Y] + k_3[B][X] - 2k_4[X]^2 \tag{13}$$

$$\frac{d[Y]}{dt} = -k_1[A][Y] - k_2[X][Y] + k_5[Z] \tag{14}$$

$$\frac{d[Z]}{dt} = k_3[B][X] - k_5[Z]. \tag{15}$$

Solutions to these differential equations will give the time-dependence of the concentration of intermediates. If we consider the reaction initiated at a single point by a metal ion catalyst, the diffusion of the reduced bromine-containing intermediates down their respective concentration gradients shows spatial dependence that results in a "target pattern".

2.3 Procedure

2.3.1 Stirred BZ Reaction (3-D)

Initially, 5 mL each of 1.5 M sodium bromate and 0.25 M sodium bromide were mixed in a beaker on a stir plate. A stir bar was spun to produce a vortex in the solution, to which 5 mL each of 1.5 M malonic acid and 0.03 M cerium(IV) ammonium nitrate in 1.76 M sulfuric acid were supposed[2] to be added. After an amber color from the production of bromine faded, leaving a colorless solution, 200 μL of 0.025 M ferroin was added. The initial concentrations of the components of this mixture are then 0.375 M bromate, 0.0625 M bromide, 0.375 M malonic acid, 0.0075 M cerium(IV) cations, 0.44 M hydronium, and 0.25 mM ferroin. We eyed the mixture and observed quick flashes of green to blue-violet punctuating a predominate red color.

Spectral measurements were taken with an Ocean Optics model USB4000 spectrometer and an LS-1 light source controlled by the SpectraSuite program, with integration time 60 ms, boxcar width 5, and scans to average 5. We continued to stir the reaction solution thourghout these measurements. First we collected a strip chart of the absorption at 415 nm, 520 nm, and 605 nm every 0.5 s for about 5 minutes. Then we set the computer to save spectra at regular intervals and collected 101 different absorption spectra.

2.3.2 Thin-Layer (2-D) BZ Reaction

Initially, 2.5 mL each of 1.5 M sodium bromate, 0.25 M sodium bromide, 1.5 M malonic acid, and 1.76 M sulfuric acid were stirred in a beaker until the amber color from the production of bromine faded, leaving a colorless solution.

[2]Both the 0.03 M cerium(IV) ammonium nitrate in 1.76 M sulfuric acid intended for the three-dimensional reaction and the plain 1.76 M sulfuric acid intended for the two-dimensional reaction were labelled "Solution D". We confused the latter for the former here. Though we finished collecting data on our mistake with time to spare, computer malfunctions prevented us from collecting spectral data on the correct reaction. Our analysis will be adjusted accordingly

To this a drop of 0.1% Triton X-100 detergent solution was added to facilitate spreading in a dish. Finally, 2 mL of 0.025 M ferroin was added. The initial concentrations of the components of this mixture are then 0.3125 M bromate, 0.052 M bromide, 0.3125 M malonic acid, 0.367 M hydronium, and 4.17 mM ferroin. This solution was poured into a thin layer covering the bottom of a petri dish. The BZ reaction was initiated by carefully dippng a piece of silver wire in at a point. A blue dot was observed at that point, which then spread into a "target pattern".

A Zeiss Telaval inverted microscope, with a 6V/30W tungsten-halogen illuminator passed through a 488±10 nm Thorlabs FL488-10 interference filter and a 5X achromat objective, was focused so the field of view was of order as wide as the distance between "target" bands. The illumination was adjusted to distinguish between the red (488 nm green light absorbed leaving a dark image), and blue (green light transmitted giving a light image) bands of the "target". More than 5000 frames of high (1280x1024) resolution black and white video of this focus was recorded to a computer using a CMOS (Thorlabs DCC1545M) video camera and the uc480 Viewer program.

The resulting video file was analysed using the ImageJ program. The frames were stacked on top of each other, and two circular areas, A and B, along the direction of propagation (in this case the Y direction through B then A) of the BZ wave were selected. The program measured the X and Y center of mass weighted with respect to the greyscale coloring of each circular area for each frame and returned a file with these data.

3 Data and Plots

3.1 Stirred BZ Reaction (3-D)

3.1.1 Kinetics

The absorption time series for the cerium catalyzed bulk BZ reaction is included below in Figure 1. This is the data obtained using a solution of 0.03 M cerium(IV) ammonium nitrate in 1.76 M sulfuric acid in accordance with the procedure.

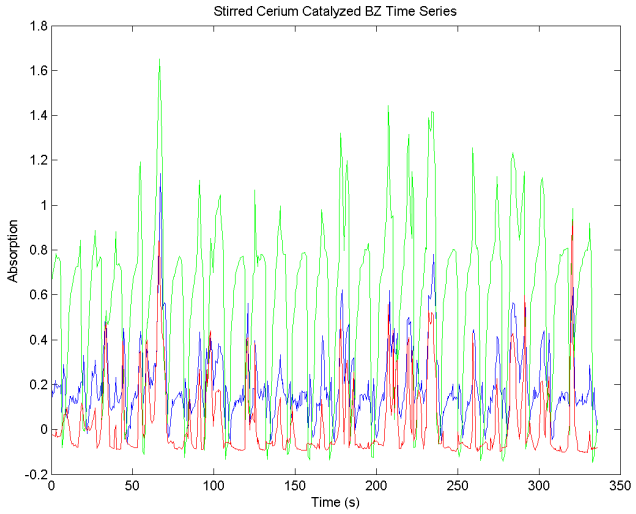

Figure 1: Absorption time series for the cerium catalyzed bulk BZ reaction for 415 nm (blue), 520 nm (green), and 605 nm (red) light.

The absorption time series for the bulk BZ reaction without the cerium catalyst is included below in Figure 2. This is the data obtained using only 1.76 M sulfuric acid. Since this data is much less noisy, and since we were unable to obtain limiting spectra for the catalyzed reaction, we will continue our analysis with this data.

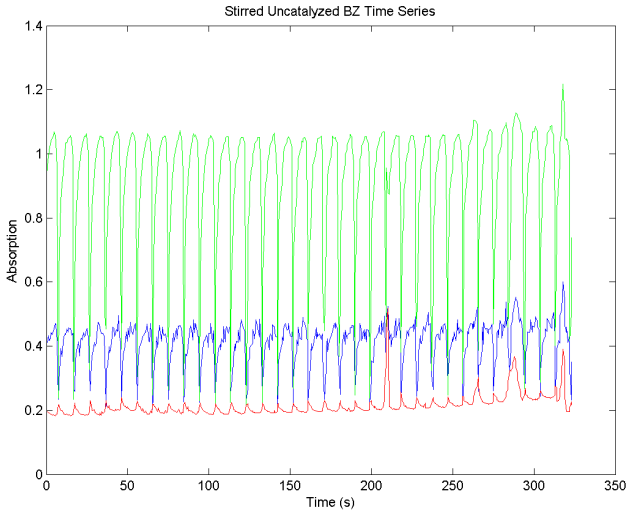

Figure 2: Absorption time series for the uncatalyzed bulk BZ reaction for 415 nm (blue), 520 nm (green), and 605 nm (red) light.

3.1.2 Unique Absorption Spectra

The primary colors visible in the bulk reaction were long periods of red interspersed with rapid flashes of aquamarine. These transmitted colors correspond to the absorption of green light and red light, respectively. It was suggested to me that the purpose of the cerium catalyst was to slow the oscillations of the reaction. Looking at the time series for the uncatalyzed reaction above in Figure reftsun, it is clear that the maximum absorption for red light is much lower than the maximum absorbance for green light. Therefore, we expect the limiting spectra, that is those for the unique appearances of red and aquamarine, to show an absorption peak around 500 nm for red, and a small peak, if any, above 600 nm for aquamarine. Of course, this assumes the reactions oscillate with the same frequency and that we were able to capture the spectra at the perfect time during the aquamarine flash. We can't assume. The unique spectra are included below as Figures 3 and 4, respectively.

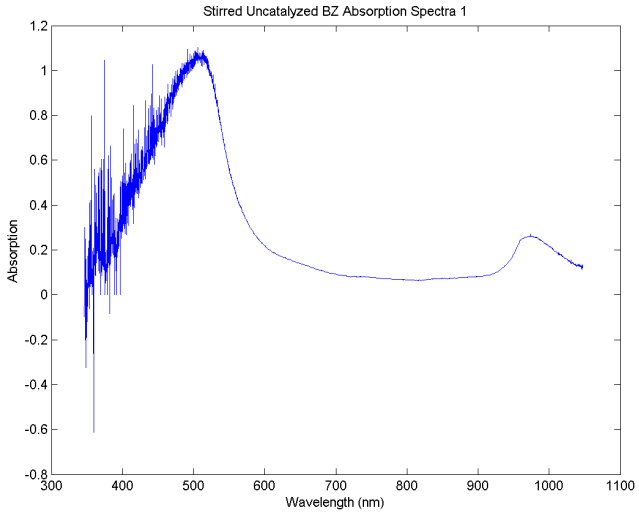

Figure 3: Limiting absorption spectra for the uncatalyzed bulk BZ reaction while appearing red.

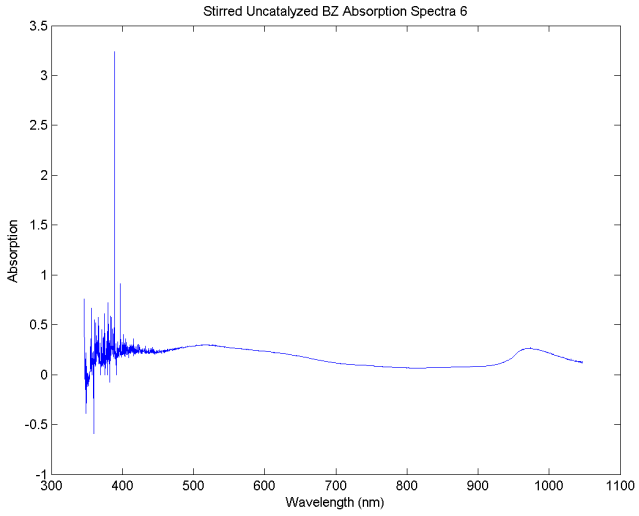

Figure 4: Limiting absorption spectra for the uncatalyzed bulk BZ reaction while appearing aquamarine.

3.2 Thin-Layer (2-D) BZ Reaction

3.2.1 Observations

The reaction wavefronts were seen to reflect off of the walls of the container. Given how slowly the wavefronts progressed, we were not really able to see the reaction cease or the thin-layer to homogenize. When we tried to do the reaction a second time, the reaction appeared to initiate on its own. This is likely the cause of residual silver left when we simply placed the wire in the second petri dish. I guess the silver necessary to initiallize the reaction is minimal. We did not collect video of this second reaction dish.

3.2.2 Frame Rate and Pixel Resolution

The video recorded was 402 seconds long and had 5618 frames, giving an average frame rate of 13.98 frames per second.

CMOS camera images in the focal plane of the 5X objective have a resolution calibrated to 3.85 pixels per μm.

3.2.3 Center of Mass

The calculated Y-direction center of mass data for circular areas A and B, adjusted by a constant for clarity and divided by the pixel resolution to give a displacement, and with the frame count vector divided by the frame rate to give time, is included below in Figure 5.

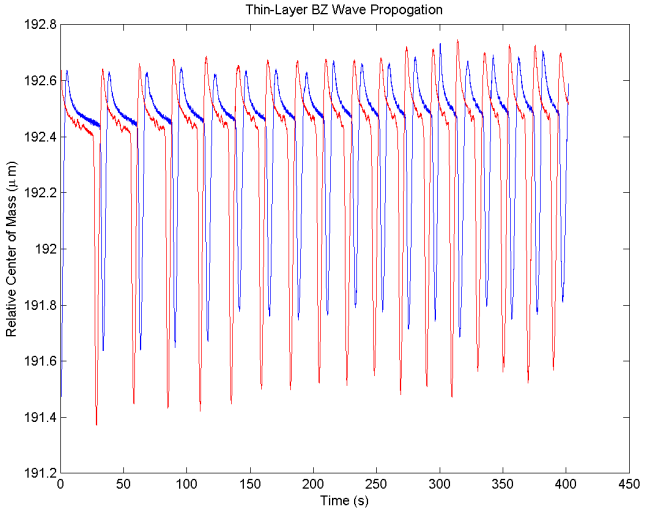

Figure 5: Relative center of mass of circular areas A (blue) and B (red) over time in thin layer BZ reaction.

4 Analysis

4.1 Lotka Mechanism Simulation

4.1.1 Numerical Solutions

Setting the constants k_1=0.01, k_2=0.03 and k_3=0.02 (all in units of sec^{-1} M^{-1}), and [A(0)]=[X(0)]=[Y(0)]=1.0 M and [P(0)]=0.0 M in the Lotka Mechanism, we solve the system of Equations (4) through (7) numerically. The result is plotted below in figure 6. Note that since we cannot solve the system analytically, the plots below may only be of approximations that get worse the farther we look from our starting point.

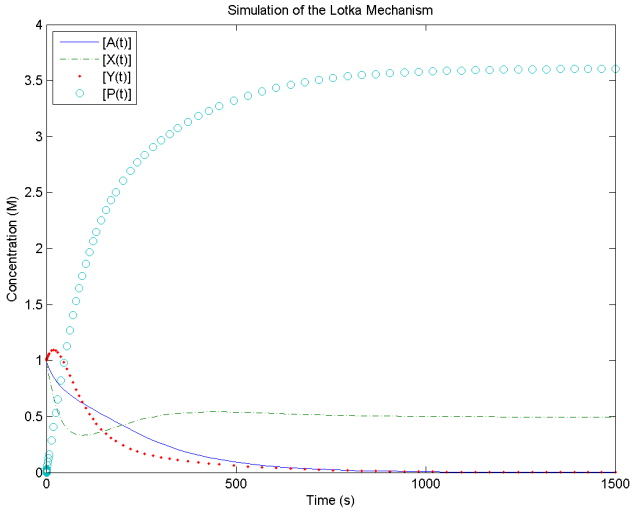

Figure 6: Time dependence of concentrations of the four species in the Lotka Mechanism.

4.1.2 Fourier Transform Analysis

The power spectra for the intermediates X and Y are included below in Figures 7 and 8. Considering the quality and quantity of simulated data available from an approximate numerical solution, these spectra are not particularly dense or distinct. They do not show any predominant frequencies. Perhaps if the rate constants and initial conditions were adjusted, or if we used a different solution method, we might get more obvious oscillations.

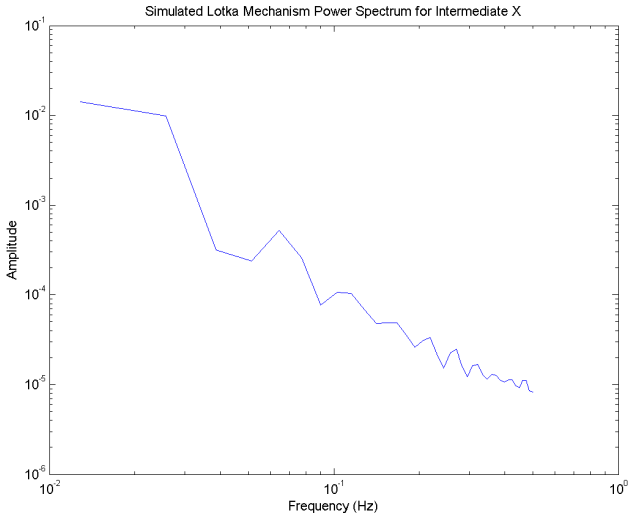

Figure 7: Power spectrum of the concentrations of the intermediate X in the Lotka Mechanism.

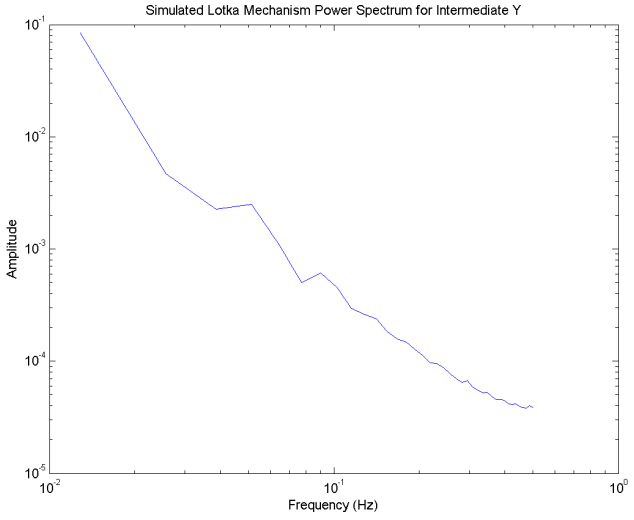

Figure 8: Power spectrum of the concentrations of the intermediate Y in the Lotka Mechanism.

4.2 Stirred BZ Reaction (3-D)

4.2.1 Fourier Transform Analysis of the Cerium Catalyzed Reaction

The power spectra of the time series for the cerium catalyzed bulk BZ reaction at all three wavelengths are included below in Figures 9, 10, and 11. The power spectrum in Figure 10 shows the most obvious irregular spikes, which have been marked with red circles. Notice that the amplitude appears to decrease linearly over regular frequency intervals on a log-log scale. Other than this, the cerium catalysed power spectra are fairly indistinct.

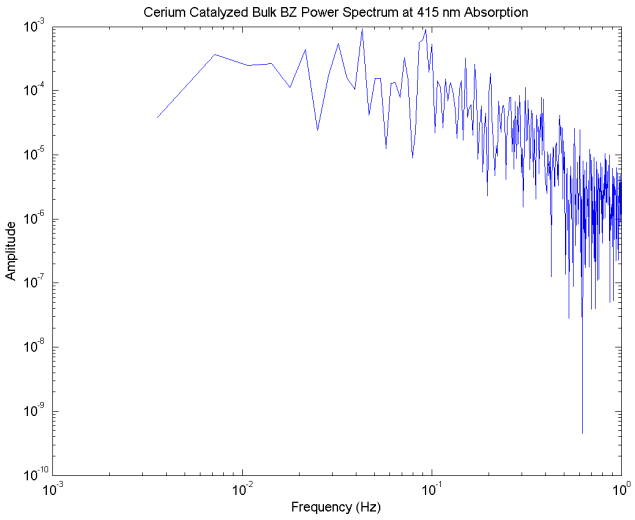

Figure 9: Power spectrum of the 415 nm time series for the cerium catalysed bulk BZ reaction.

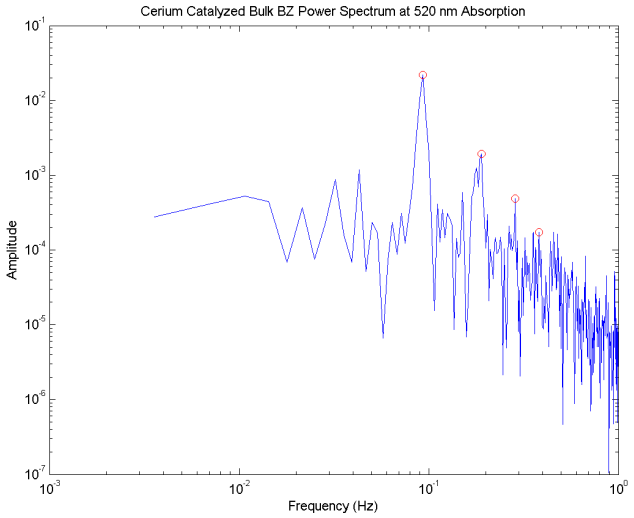

Figure 10: Power spectrum of the 520 nm time series for the cerium catalysed bulk BZ reaction with irregular spikes marked.

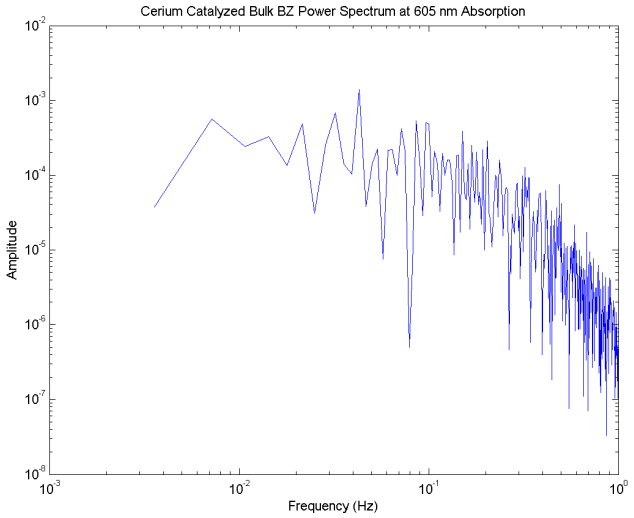

Figure 11: Power spectrum of the 605 nm time series for the cerium catalysed bulk BZ reaction.

4.2.2 Fourier Transform Analysis of the Uncatalyzed Reaction

The power spectra of the time series for the uncatalyzed bulk BZ reaction at all three wavelengths are included below in Figures 12, 13, and 14. All show obvious irregular spikes, which have been marked with red circles. Again, the amplitude appears to decrease linearly over regular frequency intervals on a log-log scale.

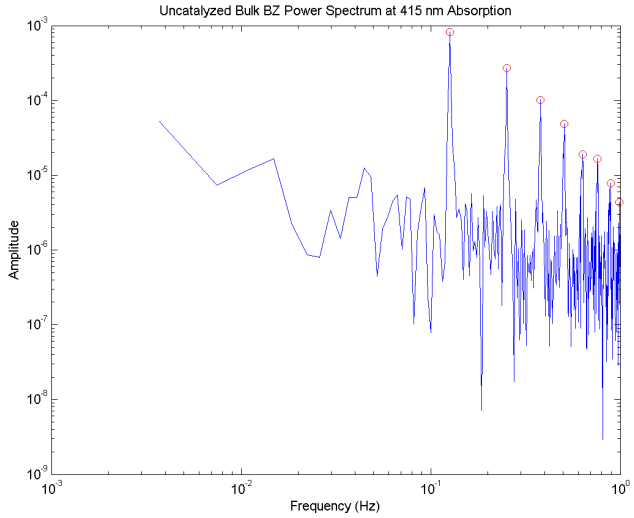

Figure 12: Power spectrum of the 415 nm time series for the uncatalysed bulk BZ reaction with irregular spikes marked.

The frequencies of the marked spikes for the spectrum in 12 are 0.126 Hz, 0.253 Hz, 0.379 Hz, 0.506 Hz, 0.632 Hz, 0.758 Hz, 0.888 Hz, and 0.993 Hz.

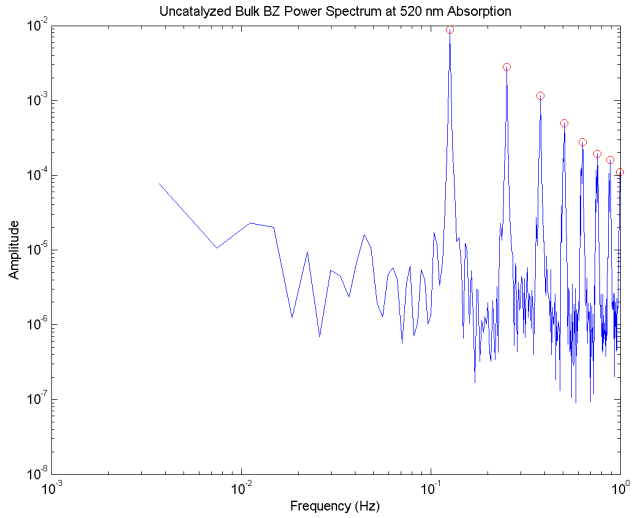

Figure 13: Power spectrum of the 520 nm time series for the uncatalysed bulk BZ reaction with irregular spikes marked.

The frequencies of the marked spikes for the spectrum in 13 are 0.126 Hz, 0.253 Hz, 0.379 Hz, 0.506 Hz, 0.632 Hz, 0.758 Hz, 0.885 Hz, and 0.996 Hz.

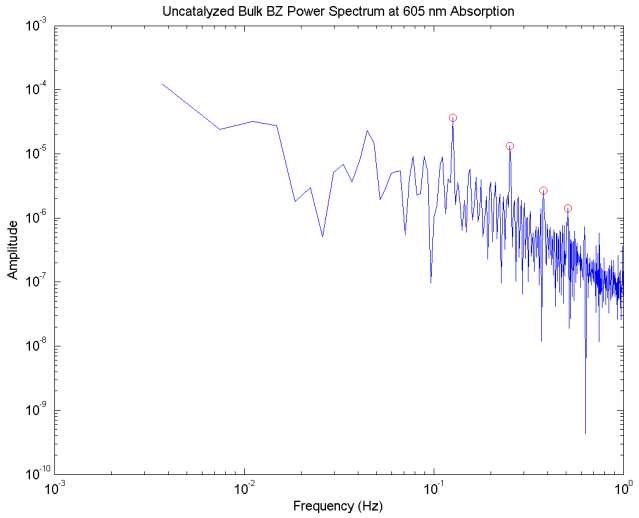

Figure 14: Power spectrum of the 605 nm time series for the uncatalysed bulk BZ reaction with irregular spikes marked.

The frequencies of the marked spikes for the spectrum in 14 are 0.126 Hz, 0.253 Hz, 0.379 Hz, and 0.509 Hz.

All of the marker frequencies fall near integer multiples of the "fundamental" frequency 0.126 Hz, that is there appear to be "open" (they are integer, and not odd integer multiples) overtones in the system.

4.3 Thin-Layer (2-D) BZ Reaction

4.3.1 Wave Propagation via Fourier Decomposition

Figure 5 suggests the passage of seventeen wavefronts over the 402 second measurement, giving an estimate of 42.2 mHz as the predominant frequency. Blips at 47.2 mHZ appear in the power spectra for both areas A and B and are marked in Figures 15 and 16 below.

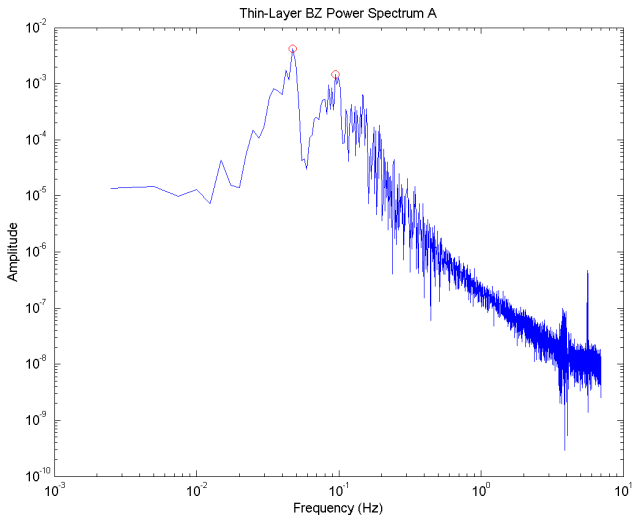

Figure 15: Power spectrum of the time trace of A for the thin-layer BZ reaction with irregular spikes marked.

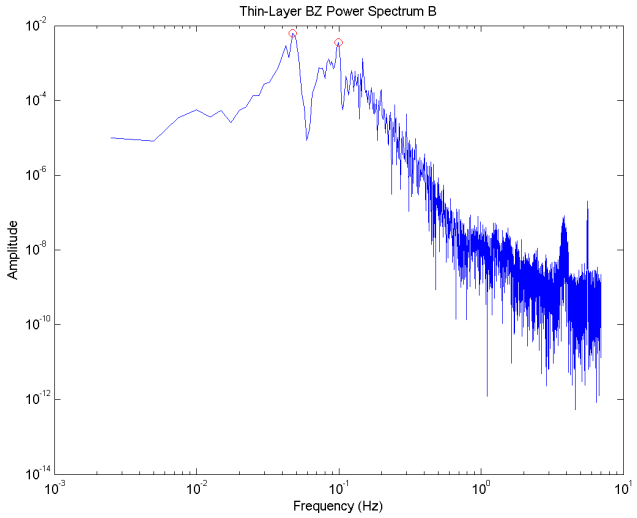

Figure 16: Power spectrum of the time trace of A for the thin-layer BZ reaction with irregular spikes marked.

Of course, these frquencies only give the number of wavefronts passing A or B per unit time. We need the distance from A to B and the time between wavefront passages to get a velocity.

Watching the video recorded with the CMOS camera again, we seem the passage of a light front, corresponding to the increased transmittance of 488 nm green light, across the screen from B to A in a period of about six seconds, interspersed with a longer period of darkness, corresponding to low transmittance of 488 nm green light. Looking again at Figure 5, we understandt why the red spikes for B come so much closer to the following blue spikes for A, rather than the preceeding. With this information, we can query the time between consecutive spikes, i.e. wavefronts. Now understanding which spikes correspond to the same wavefront, we can query the distance between the unadjusted center of mass spikes to get an estimate of the distance from A to B.

The average time for passage of a wavefront from B to A over seventeen wavefronts is 6.36 seconds with a standard of deviation of 0.83 seconds. The average distance between the wavefront spikes at B and A over seventeen wavefronts is 147.38 μm with a standard of deviation 0.02 μm. This gives an average velocity with less than 2% uncertainty of 23.2 μm per second.

4.3.2 Theoretical Wavefront Velocity

It has been experimentally determined by Field and Noyes that the wavefront velocity is related to the hydronium and bromate concentrations as

$$\mathrm{v} = \mathrm{k}[\mathrm{H}^+]^{1/2}[\mathrm{BrO}_3^-]^{1/2}, \tag{16}$$

where the rate constant k=0.04 cm sec^{-1} M^{-1}. Further, the wavefront the result of the diffusion of concentration gradients, so its propagation depends on the directions available for diffusion. The result of this is that in thin-layer solution, the velocity of a wavefront initiated at a point depends on curvature as

$$v^* = v + DK, \tag{17}$$

where D is the diffusion coefficient on the order of 10^{-5} cm^2 sec^{-1}, and $K = \pm r^{-1}$, positive for a contracting wave and negative for expanding. Now, we have approximated the distance between A and B assuming linear propagation of the wavefront, neglecting the curvature. This should be of little harm as long as we correctly assigned the wavefronts.

Using equations (16) and (17) with the concentrations from the procedure above, the given values for the rate and diffusion coefficients, and taking $r \approx 3$ cm for a 60 mm perti dish, we calculate a velocity of 135 μm per second. There is an order of magnitude discrepancy between the two wavefront velocities.

5 Discussion

5.1 Oscillatory Kinetics

Neither by looking at the power spectra, nor by looking at the data in Figure 2 am I able to discern a damper in the bulk reaction. Thus, I cannot come up with a relaxation time. Further, since I see no damping, I do not know if after the reaction has reached equilibrium (which I know it must by the Second Law of Thermodynamics), if the reaction can be regenerated. It would certainly be novel if there was a much lower frequency by which the reaction appeared to damp to equilibrium, but then regenerated itself, or if it reached steps of equilibrium and the intermediates just needed to be perturbed between each step to get the reaction to progress. The same goes for the thin-layer reaction, though in all likelyhood if I had simply observed the reaction for longer, I would have seen some damping as the wavefronts interfered with each other. This holds even though the waves would have reinforced each other at some points; the thin layer solution was not controlled enough for us to get, say, diffraction patterns, though that would be cool to try.

5.2 Wave Phenomena

There is an order of magnitude discrepancy between the wavefront velocity calculated from theory. and from time trace data. Perhaps in the theory we have made an assumption about the diffusion that we shouldn't have. We need to account for the diffusion of intermediates down their concentration gradients. If these gradients point in opposite directions for two different intermediates, then maybe we should not simply concatenate equations (16) and (17).

The propogation of the BZ reaction wavefront in thin-layer solution depends upon the diffusion of particles down concentration gradients into a position to

produce sufficient inhomogeneity of particles and also to bring reacting species together. These are not simple waves. Similarly, waves in water depend upon the diffusion of particles affected by different forces like hydrogen bonds, forces from other dissolved particles, and inhomogeneities in pressure and temperature. Though propagation speed in light waves may be determined from wavelength and the media through which it passes, water and BZ waves are the media, and therefore are not so simple. This is likely why they dissipate the way they do; self interference damps things out. This is also probably why I have never seen a standing wave in water, and suggests that a perturbation of some sort is absolutely necessary to regenerate the BZ reaction if it damps to equilibrium.

5.3 Conclusions

This lab has emphasized the parallels between the chemical and physical as schema and not just natural phenomena. The concept of waves and oscillations in a chemical reaction that I can actually see suggests new ways to think of complex processes like the rolling of the ocean waves.

It would be fun to try to pass a thin-layer BZ wavefront through a diffreaction grating to see if we could get a distinct interference pattern.